UICC
global cancer control

IJC
International Journal of Cancer

The antitumor activity of the fungicide ciclopirox

Hongyu Zhou[1], Tao Shen[1], Yan Luo[1], Lei Liu[1], Wenxing Chen[1], Baoshan Xu[1], Xiuzhen Han[1], Jia Pang[2], Chantal A. Rivera[2] and Shile Huang[1,3]

[1] Department of Biochemistry and Molecular Biology, Louisiana State University Health Sciences Center, Shreveport, LA
[2] Department of Molecular and Cellular Physiology, Louisiana State University Health Sciences Center, Shreveport, LA
[3] Feist-Weiller Cancer Center, Louisiana State University Health Sciences Center, Shreveport, LA

Ciclopirox olamine (CPX) is a synthetic antifungal agent clinically used to treat mycoses of the skin and nails. Here, we show that CPX inhibited tumor growth in human breast cancer MDA-MB-231 xenografts. To unveil the underlying mechanism, we further studied the antitumor activity of CPX in cell culture. The results indicate that CPX inhibited cell proliferation and induced apoptosis in human rhabdomyosarcoma (Rh30), breast carcinoma (MDA-MB231) and colon adenocarcinoma (HT-29) cells in a concentration-dependent manner. By cell cycle analysis, CPX induced accumulation of cells in G_1/G_0 phase of the cell cycle. Concurrently, CPX downregulated cellular protein expression of cyclins (A, B1, D1 and E) and cyclin-dependent kinases (CDK2 and CDK4) and upregulated expression of the CDK inhibitor $p21^{Cip1}$, leading to hypophosphorylation of retinoblastoma protein. CPX also downregulated protein expression of Bcl-xL and survivin and enhanced cleavages of Bcl-2. Z-VAD-FMK, a pan-caspase inhibitor, partially prevented CPX-induced cell death, suggesting that CPX-induced apoptosis of cancer cells is mediated at least in part through caspase-dependent mechanism. The results indicate that CPX is a potential antitumor agent.

Ciclopirox olamine (CPX) (also called Batrafen, Loprox, Penlac and Stieprox), the ethanolamine salt of 6-cyclohexyl-1-hydroxy-4-methyl-2(1H)-pyridone, is a synthetic antifungal agent used to treat mycoses of the skin and nails for more than 20 years.[1–3]

Studies have shown that CPX has a very broad spectrum of action against dermatophytes, yeast, filamentous fungi and bacteria.[4,5] The mechanisms of these actions of CPX seem diverse, involving disruption of membrane function in fungi or targeting different metabolic (respiratory) and energy-producing processes in bacteria.[1,2] In the yeast *Saccharomyces cerevisiae*, CPX may also exert its effect by disrupting DNA repair, cell division signals and structures (mitotic spindles) as well as some elements of intracellular transport.[6] Apart from its antimycotic and antibacterial activities, CPX arrests the cell cycle at G_1 phase in mammalian cells[7,8] and G_2/M phase in the yeast *S. cerevisiae*.[9] CPX also prevents the death of tropic factor-deprived PC12 cells and postmitotic sympathetic neurons by blocking the cell cycle progression[7] or the death of cerebellar granule neurons in low K^+-containing medium,[10] but it induces an active cell death in *S. cerevisiae*.[9]

In addition, CPX is a well-known iron chelator, inhibiting the iron-containing enzymes, such as catalase and peroxidase.[11] Most recent studies have revealed that the chelation of intracellular iron and the inhibition of the iron-dependent enzyme ribonucleotide reductase were associated with CPX-induced cell death.[12] It appeared that CPX induced cell death in primary human acute myeloid leukemia (AML) cells and inhibited engraftment of primary AML cells in NOD/SCID mouse models without gross organ toxicity or loss of body weight.[12] Previous safety and toxicity studies of CPX also demonstrated that a 4-week oral administration of 30 mg/kg body weight and a 3-month administration of 10 mg/kg produced no toxicity, revealing a favorable therapeutic index of CPX.[13] Based on these findings, it will be interesting to investigate whether CPX displays preclinical anticancer activity against solid tumors, such as rhabdomyosarcoma, breast cancer, prostate cancer and colon cancer.

To provide a further preclinical rationale for the development of CPX as an anticancer agent, we initiated this study to test the *in vivo* effect of CPX against human breast cancer MDA-MB231 tumor growth in a mouse xenograft model. Our results show that CPX potently inhibited the tumor growth by inhibiting proliferation and inducing apoptosis of the tumor cells *in vivo*. This is further supported by our *in vitro* findings. By cell cycle analysis, CPX induced accumulation of the cancer cells in G_1/G_0 phase of the cell cycle. Concurrently, we observed that CPX inhibited cellular

Key words: ciclopirox, cell proliferation, cell cycle, apoptosis, retinoblastoma protein
Grant sponsor: NIH; **Grant number:** CA115414; **Grant sponsor:** American Cancer Society Award; **Grant number:** RSG-08-135-01-CNE; **Grant sponsor:** Louisiana State University Health Sciences Center in Shreveport, LA (Feist-Weiller Cancer Research Award and a Start-up Fund)
DOI: 10.1002/ijc.25255
History: Received 14 Jan 2010; Accepted 2 Feb 2010; Online 11 Mar 2010
Correspondence to: Shile Huang, Department of Biochemistry and Molecular Biology, Louisiana State University Health Sciences Center, 1501 Kings Highway, Shreveport, LA 71130-3932, USA, Fax: +318-675-5180, E-mail: shuan1@lsuhsc.edu

protein expression of cyclins (A, B1, D1 and E) and CDKs (CDK2 and CDK4) and increased expression of the CDK inhibitor $p21^{Cip1}$, leading to decreased phosphorylation of retinoblastoma (Rb). CPX also increased caspase-3/7 activity, downregulated protein expression of Bcl-xL and survivin and enhanced cleavages of Bcl-2 and poly (ADP-ribose) polymerase (PARP). Z-VAD-FMK, a pan-caspase inhibitor, partially prevented CPX-induced cell death, suggesting that CPX-induced apoptosis of cancer cells is at least in part mediated through caspase-dependent mechanisms.

Material and Methods

Materials

CPX (Sigma, St. Louis, MO) was dissolved in 100% ethanol to prepare a stock solution (100 mM), then aliquoted and stored at −20°C. RPMI 1640 and Dulbecco's Modified Eagle Medium (DMEM) were purchased from Mediatech (Herndon, VA). Fetal bovine serum (FBS) was from Hyclone (Logan, UT) and 0.05% Trypsin-EDTA was from Invitrogen (Grand Island, NY). Enhanced chemiluminescence solution was obtained from PerkinElmer Life Science (Boston, MA). The following primary antibodies were used, including those against cyclin A, cyclin B1, cyclin D1, cyclin E, CDK2, CDK4, Rb, $p21^{Cip1}$, $p27^{Kip1}$, survivin, Bcl-2, Ki-67 (Santa Cruz Biotechnology, Santa Cruz, CA), BAK, BAX, Bcl-xL (Biomeda, Foster, CA), BAD, PARP (Cell Signaling, Beverly, MA) and β-tubulin (Sigma, St. Louis, MO). Goat anti-mouse IgG-horseradish peroxidase (HRP) and goat anti-rabbit IgG-HRP were purchased from Pierce (Rockland, IL).

Cell lines and cultures

Human rhabdomyosarcoma (Rh30) (expressing mutant *p53* alleles R273C, a gift from Dr. Peter J. Houghton, St. Jude Children's Research Hospital, Memphis, TN) was grown in antibiotic-free RPMI 1640 medium supplemented with 10% FBS at 37°C and 5% CO_2. Human breast carcinoma (MDA-MB231, expressing mutant *p53* alleles R280K) and human colon cancer (HT-29, expressing mutant *p53* alleles R273H) cells (American Type Culture Collection, Manassas, VA) were grown in antibiotic-free DMEM supplemented with 10% FBS at 37°C and 5% CO_2. In all treatments, CPX was dissolved in 100% ethanol to prepare a stock solution (100 mM). The subconfluent cells (60–70% confluent) were treated with varying concentrations of CPX in complete cell culture medium. Cells treated with vehicle (ethanol, final concentration in media = 0.1%) served as a control.

Cell morphological analysis

Cells were seeded in 6-well plates at a density of 3×10^5 cells per well under standard culture conditions and kept overnight at 37°C humidified incubator with 5% CO_2. The next day, the cells were treated with CPX (0–20 μM). After incubation for 48 hr, images were taken with an Olympus inverted phase-contrast microscope (Olympus Optical, Melville, NY) equipped with the Quick Imaging system. For experiments with a pan-caspase inhibitor, the cells were pre-incubated without or with Z-VAD-FMK (10 μM) for 30 min and then treated without or with CPX (20 μM) for 48 hr. The cells were photographed with an Olympus inverted phase-contrast microscope (200×) equipped with Quick Imaging System.

Cell proliferation assay

Cells were seeded in 6-well plates at a density of 3×10^5 cells/well (in triplicate) under standard culture conditions and kept overnight at 37°C humidified incubator with 5% CO_2. The next day, the cells were treated with CPX (0–20 μM) for 48 hr or exposed to CPX (10 μM) for 0–6 days. After incubation, the cells were harvested after trypsinization and then counted with a Beckman Coulter Counter (Beckman Coulter, Fullerton, CA).

Cell cycle analysis

Cell cycle analysis was performed as described previously.[14] Briefly, cells were seeded in 6-well plates at a density of 8×10^5 cells/well under standard culture conditions and kept overnight at 37°C humidified incubator with 5% CO_2. The next day, the cells were treated with CPX (0–20 μM) for 24–48 hr. The cells were then trypsinized, washed with cold phosphate-buffered saline (PBS) and processed for cell cycle analysis using Cellular DNA Flow Cytometric Analysis Kit (Roche Diagnostics Corp., Indianapolis, IN) according to the manufacturer's instructions. Cells treated with vehicle alone (100% ethanol) were used as a control.

Apoptosis assay

Apoptosis assay was performed as described previously.[14] Briefly, cells were seeded in 6-well plates at a density of 6×10^5 cells/well under standard culture conditions and kept overnight at 37°C humidified incubator with 5% CO_2. The next day, the cells were treated with CPX (0–20 μM) for 48 hr. The cells were then trypsinized, washed with cold PBS and processed for apoptosis assay using the Annexin V-FITC Apoptosis Detection Kit I (BD Biosciences, San Diego, CA) by following the instructions of the manufacturer. Cells treated with vehicle alone (100% ethanol) were used as a control.

Western blot analysis

Cells were seeded in 6-well plates at a density of 6×10^5 cells/well under standard culture conditions and kept overnight at 37°C humidified incubator with 5% CO_2. The next day, the cells were treated with CPX (0–20 μM) for 24 hr or with 20 μM CPX for 0–24 hr. Subsequently, cells were briefly washed with cold PBS and lysed in RIPA buffer [50 mM Tris, pH 7.2; 150 mM NaCl; 1% sodium deoxycholate; 0.1% SDS; 1% Triton-X 100; 10 mM NaF; 1 mM Na_3VO_4; protease inhibitor cocktail (1:1,000, Sigma, St. Louis, MO)]. Cell lysates were sonicated for twice, 10 sec each time, and then centrifuged at 13,000 rpm for 10 min at 4°C. Protein

concentration was determined by bicinchoninic acid assay with bovine serum albumin as standard (Pierce, Rockford, IL). Equivalent amounts of protein were separated on 8–12% SDS-polyacrylamide gel and transferred to polyvinylidene difloride membranes (Millipore, Bedford, MA). Membranes containing the transferred protein were incubated in blocking buffer (PBS containing 0.1% Tween-20 and 5% nonfat dry milk) for 1 hr at room temperature to block nonspecific binding and then incubated with appropriate primary antibodies followed by incubation with anti-mouse or anti-rabbit secondary antibodies conjugated to HRP. Immunoreactive bands were visualized by using Renaissance chemiluminescence reagent (Perkin-Elmer Life Science, Boston, MA). To check the amount of protein loaded, the immunoblots were treated with stripping solution (62.5 mM Tris buffer, pH 6.7, containing 2% SDS and 100 mM 2-mercaptoethanol) for 30 min at 50°C and incubated with mouse monoclonal anti-β-tubulin antibody (Sigma) followed by HRP-coupled goat anti-mouse IgG (Pierce).

Caspase-3/7 activity assay

Cells were seeded in 96-well black plates at a density of 1×10^4 cells/well under standard culture conditions and kept overnight at 37°C humidified incubator with 5% CO_2. The next day, the cells were preincubated without or with Z-VAD-FMK (10 μM) for 30 min and then treated without or with CPX (0–20 μM) for 24 hr. Caspase-3/7 activity was measured using the SensoLyte Homogeneous AMC Caspase 3/7 Assay kit (AnaSpec, Fremont, CA) according to the manufacturer's protocol. In brief, 50 μl/well of caspase-3/7 substrate solution was added into each well. After 12-hr incubation at room temperature, the fluorescence intensity was measured by excitation at 355 nm and emission at 460 nm using a Wallac 1420 Multilabel Counter (PerkinElmer Life Sciences, Wellesley, MA). Caspase-3/7 activity was indicated as relative fluorescence units.

In vivo analysis of anticancer effect of CPX

BALB/c *nu/nu* mice (Harlan, Indianapolis, IN) were randomly grouped (5 mice/group). Human breast carcinoma (MDA-MB231) cells were chosen for the xenogaft studies, because the cell line was found to be sensitive to CPX in culture. MDA-MB231 cells (2×10^6, resuspended in PBS) were subcutaneously injected into both flanks of the mice. Seven days later, mice were then treated daily by oral gavages with CPX (25 mg/kg) prepared in a solution (4% ethanol, 5.2% Tween 80 and 5.2%PEG 400) or vehicle control. The dose used was based on studies with CPX on leukemia xenograft experiments.[12] Tumor volume [(length × width^2)/2] was determined with a digital caliper. At the end of experiments, animals were sacrificed, and the tumors were collected for further analysis. All procedures were carried out in accordance with the guidelines of the Institutional Animal Care and Use Committee and were in compliance with the guidelines set forth by the Guide for the Care and Use of Laboratory Animals.

Immunohistochemistry

Tumor tissues were excised and fixed with 10% formalin, embedded in paraffin and sectioned using a standard histological procedure. For overall morphological observations, the tissue sections were stained with hematoxylin and eosin (H&E). For Ki-67 staining, paraffin sections were deparaffinized in xylene and hydrated in decreasing grades of ethanol. The slides were immersed in 3% hydrogen peroxide (Sigma) for 20 min to block endogenous peroxidase activity and then washed in PBS. For antigen retrieval, the slides were placed in preheated working solution of Retrievagen A (BD Pharmingen, San Jose, CA) and heated in a steamer for 70 min. After cooling for 20 min at room temperature, slides were rinsed with PBS and then treated with 10% normal FBS for 30 min, followed by incubation with rabbit anti-Ki-67 antibodies for 2 hr. Slides were then washed with PBS and incubated with the HRP-labeled goat anti-rabbit IgG antibodies for 1 hr at room temperature. After washing with PBS, a streptavidin-HRP (BD Pharmingen) was added and incubated for 30 min. Slides were then stained with 3,3′-diaminobenzidine (Vector Laboratories, Burlingame, CA) for 3 min. Counterstaining was performed with hematoxylin (Vector Laboratories). After washing with distilled water, the slides were dehydrated in increasing grades of ethanol, cleared with xylene and mounted using permanent mounting medium (Vector Laboratories). The proliferation index was determined by measuring the percentage of Ki-67-positive cells. A total of 15 randomly selected fields at 20× magnification from 3 tumors of each treatment group were examined.

TUNEL assay

The TUNEL assay was performed by using DeadEnd Colorimetric TUNEL System (Promega, Madison, WI) following the manufacturer's instructions. In brief, tissue sections were deparaffinized, rehydrated and washed as described above, followed by treatment with 20 μg/ml of proteinase K for 10 min at room temperature. After washing and equilibrating, rTdT reaction mix was added on the sections. Slides were then covered with plastic coverslips and incubated for 60 min at 37°C in a humidified atmosphere. The reaction was terminated with a stop buffer, and endogenous peroxidase activity was blocked with 0.3% hydrogen peroxide for 5 min. After washing with PBS, the sections were incubated with streptavidin-HRP for 30 min, washed with PBS, stained with 3,3′-diaminobenzidine and mounted. The apoptotic index was determined by counting the total number of positive nuclei in 15 randomly selected fields at 20× magnification.

Statistical analysis

The results were expressed as mean values ± standard deviation (mean ± SD). Statistical analysis was performed by

Student's *t*-test (STATISTICA, Statsoft, Tulsa, OK). A level of $p < 0.05$ was considered to be significant.

Results

CPX inhibits tumor growth in human breast cancer MDA-MB231 xenografts in mice

To assess the antitumor effect of CPX, human breast cancer MDA-MB231 xenografts were established in BALB/c *nu/nu* mice. When tumors reached <200 mm^3, mice were divided randomly into CPX treatment group and control group (5 mice/group). Subsequently, mice were treated daily by oral gavages with CPX (25 mg/kg) prepared in a solution (4% ethanol, 5.2% Tween 80 and 5.2% PEG 400) or vehicle control. At the end of 24 days, control tumors grew to an average size of 1,692 ± 375 mm^3 (Fig. 1). CPX-treated tumors grew to 400 ± 52 mm^3, showing ~75% tumor growth inhibition. The results indicate that CPX is a potential antitumor agent.

To determine whether CPX inhibited the tumor growth through inhibition of tumor cell proliferation and/or induction of tumor cell apoptosis, at the end (Day 24) of the *in vivo* experiments, all MDA-MB231-xenografted mice were sacrificed. Tumors were excised from the animals, followed by H&E staining, Ki-67 staining and TUNEL staining. As shown in Figure 2*a*, CPX inhibited proliferation of MDA-MB231 cells in mouse-xenografted tumors by ~63%. Besides, CPX also induced remarkable apoptosis of the cells (Fig. 2*b*).

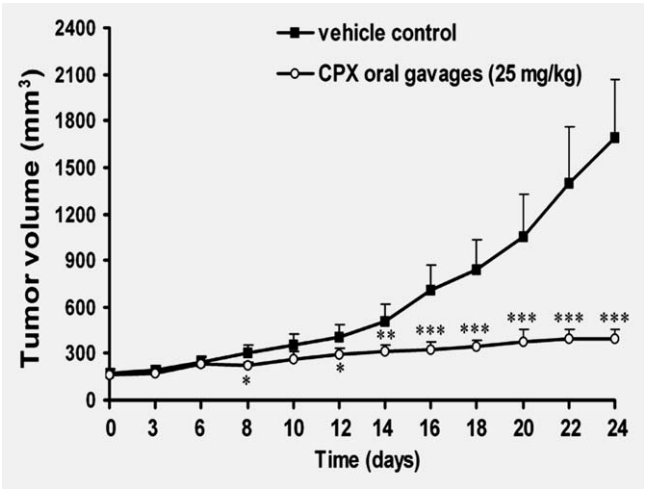

Figure 1. CPX inhibits tumor growth in human breast cancer MDA-MB231 xenografts in mice. Nude mice bearing MDA-MB231 xenografts were treated daily by oral gavages with CPX (25 mg/kg) as described in Material and Methods. Tumor volume was measured at indicated time (days). Results are presented as mean ± SD ($n = 5$). *$p < 0.05$, **$p < 0.01$, ***$p < 0.001$, difference *versus* vehicle-treated control group.

CPX inhibits tumor cell proliferation

To further unveil the mechanism by which CPX inhibits the tumor growth, we extended our studies in cell culture model. First, we investigated the effect of CPX on tumor cell proliferation. As shown in Figures 3*a* and 3*b*, treatment with CPX (0–20 μM) for 48 hr inhibited proliferation of MDA-MB231 cells in a concentration-dependent manner. Similar results were also observed in human rhabdomyosarcoma (Rh30) and colon adenocarcinoma (HT-29) cells, with IC_{50} = 2–5 μM, suggesting that this is not a cell-type context. Under a phase-contrast microscope, we observed that CPX not only exhibited a cytostatic effect at low micromolar concentrations but also exerted a cytotoxic effect at the higher micromolar concentrations, as the original 5×10^4 seeded cells almost died out at 20 μM concentration of CPX after exposure for 6 days (data not shown).

CPX slows down cell cycle progression from G_1/G_0 to S phase in tumor cells

Cell proliferation is controlled by the progression of the cell cycle.[15] To understand how CPX inhibits cell proliferation, we assessed the effect of CPX on cell cycle distribution using propidium iodide staining and flow cytometry. As shown in Figure 4*a*, CPX (10 μM, 24 hr) effectively accumulated Rh30 cells in the G_1/G_0 phase of the cell cycle. CPX treatment significantly increased the proportion of the cells in the G_1/G_0 phase from 40.09 to 62.39% (Fig. 4*b*). This increase in G_1/G_0 cell population was accompanied with a concomitant decrease of cell number in S phase and G_2/M phase of the cell cycle. However, prolonged treatment with CPX at 10 μM resulted in 52.69% of the cells in G_1/G_0 phase, 40.53% in S phase and 6.78% in G_2/M phase (data not shown), suggesting that CPX did not completely arrest the cells in G_1/G_0 phase, but only slowed down cell cycle progression. Interestingly, when the cells were treated for 48–72 hr, a low concentration (5 μM) of CPX was able to induce a similar cell cycle accumulating effect observed at a high concentration (10 μM) for 24 hr (data not shown). Similar result was observed in MDA-MB231 cells (data not shown), indicating that CPX inhibition of cell proliferation is associated with slowing down of the cell cycle progression from G_1/G_0 to S phase.

CPX induces apoptosis in tumor cells

To verify the apoptotic effect of CPX seen in tumor xenografts, we performed annexin-V-FITC and propidium iodide staining for cultured cells. The extent of apoptosis was analyzed using FacsDiva software (BD Bioscience, San Jose, CA), following the fluorescence-activated cell sorting by flow cytometry. The late and early apoptotic cells, which are shown, respectively, in the upper right and lower right quadrants of the histograms, were counted as apoptotic cells. As shown in Figure 5*a*, treatment of Rh30 cells with CPX for 48 hr increased the percentage of apoptotic cells in a concentration-dependent manner. At 20 μM, CPX increased apoptosis by ~5-fold (Fig. 5*b*). Similar results were obtained in MBA-MD231 cells (data are not shown). Taken together, our *in vivo* and *in vitro* data support the notion that CPX can potently induce apoptosis of tumor cells.

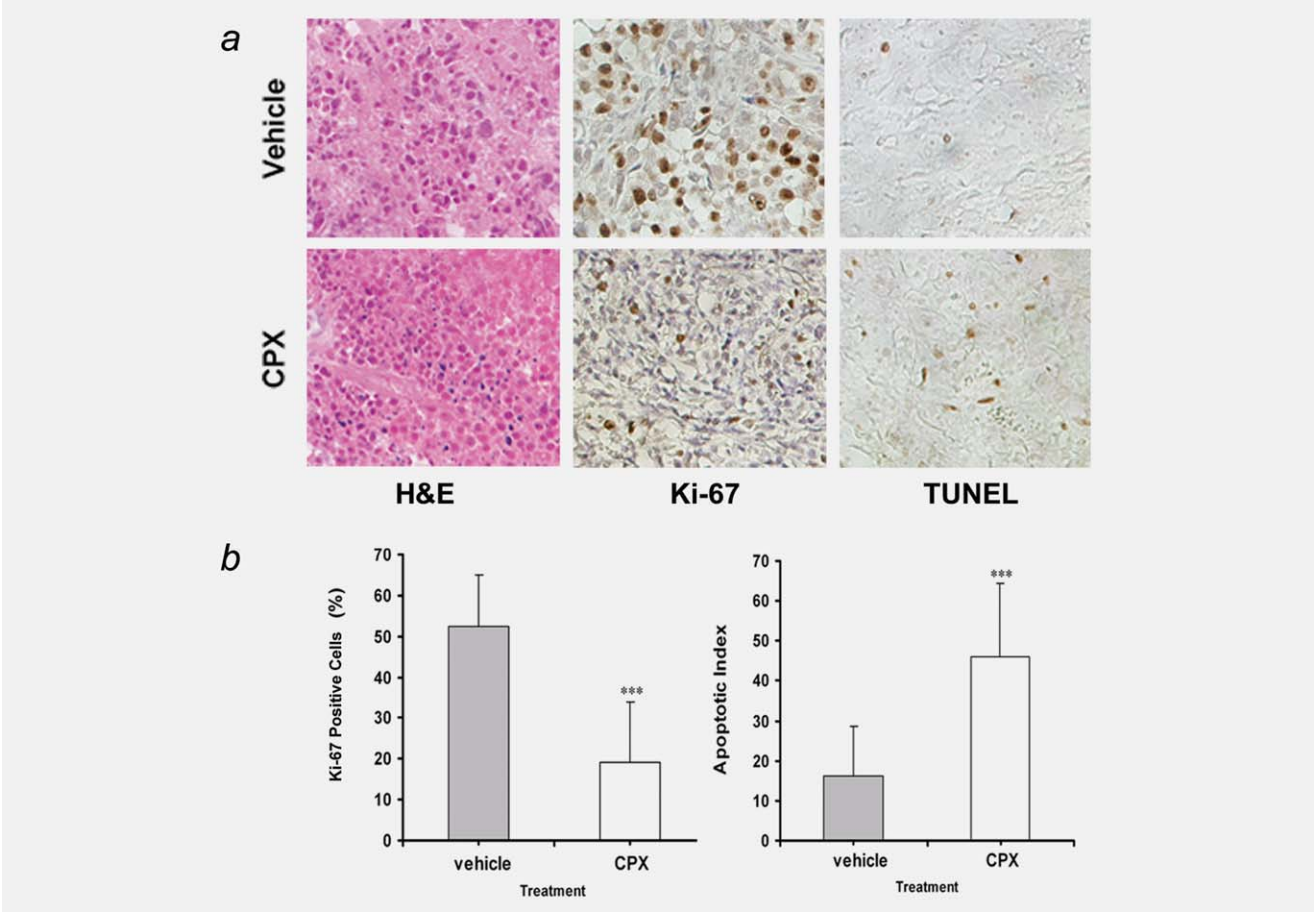

Figure 2. CPX inhibits proliferation and induces apoptosis of MDA-MB231 cells in xenografts. At the end (Day 24) of the *in vivo* experiments, all MDA-MB231-xenografted mice were sacrificed. Tumors were removed from the animals, followed by H&E staining, Ki-67 staining and TUNEL staining, as described in Material and Methods. (*a*) Representative slides of H&E staining, Ki-67 staining and TUNEL staining for MDA-MB231 tumor xenografts treated with vehicle or CPX (25 mg/kg) as described in Material and Methods. (*b*) Quantitative results (mean ± SD, $n = 3$) show Ki-67 staining and TUNEL staining in (*a*). ***$p < 0.001$, difference *versus* vehicle-treated control group.

CPX inhibits expression of cyclins, CDKs and phosphorylation of Rb in tumor cells

Cyclins and CDKs play an essential role in the regulation of cell cycle progression.[15] Thus, perturbation of cyclins or CDKs expression may contribute to the altered cell cycle distribution. Of the cell cycle-related cyclins, cyclins D and E play an important role in the transition from the G_1 to S phase, and cyclin D1-CDK4/6 and cyclin E-CDK2 complexes are required for G_1 progression.[16] To elucidate how CPX induces G_1/G_0 cell cycle accumulation, next we examined protein expression of cyclin A, cyclin B1, cyclin D1, cyclin E, CDK2 and CDK4. As shown in Figure 6*a*, treatment of Rh30 cells with CPX for 24 hr inhibited cellular protein expression of cyclin A, cyclin B1, cyclin D1, cyclin E, CDK2 and CDK4 in a concentration-dependent manner. As Rb, one of the most important G_1 phase cyclin/CDK substrates, functions as an archetypal tumor suppressor and a regulator of cell cycle progression in the late G_1 phase,[17] we investigated the effect of CPX on Rb phosphorylation. As shown in Figure 6*a*, Rb was expressed as a 110-kDa band on Western blotting in vehicle-treated control cells. After 20 μM CPX treatment for 24 hr, a lower band, which migrates rapidly and represents the dephosphorylated protein, was observed, suggesting that CPX inhibits phosphorylation of Rb, which was confirmed by Western blotting using the antibodies against p-Rb (S780 and S807) (Fig. 6*a*).

CPX upregulates expression of CDK inhibitor $p21^{Cip1}$

$p21^{Cip1}$ and $p27^{Kip1}$ are 2 major inhibitors of cyclin/CDK complexes, which can form a complex with cyclins and CDKs, inhibiting CDK activity and regulating the progression of cells in the G_1/G_0 phase of the cell cycle.[18,19] Induction of $p21^{Cip1}$ and $p27^{Kip1}$ causes a blockade of the G_1 to S transition, thereby resulting in a G_1 phase arrest of the cell cycle.[18–20] Thus, we reasoned that CPX may accumulate the cell cycle in G_1/G_0 phase by increasing the levels of these proteins. To our surprise, treatment with CPX for 16 hr markedly increased $p21^{Cip1}$ expression but slightly decrease

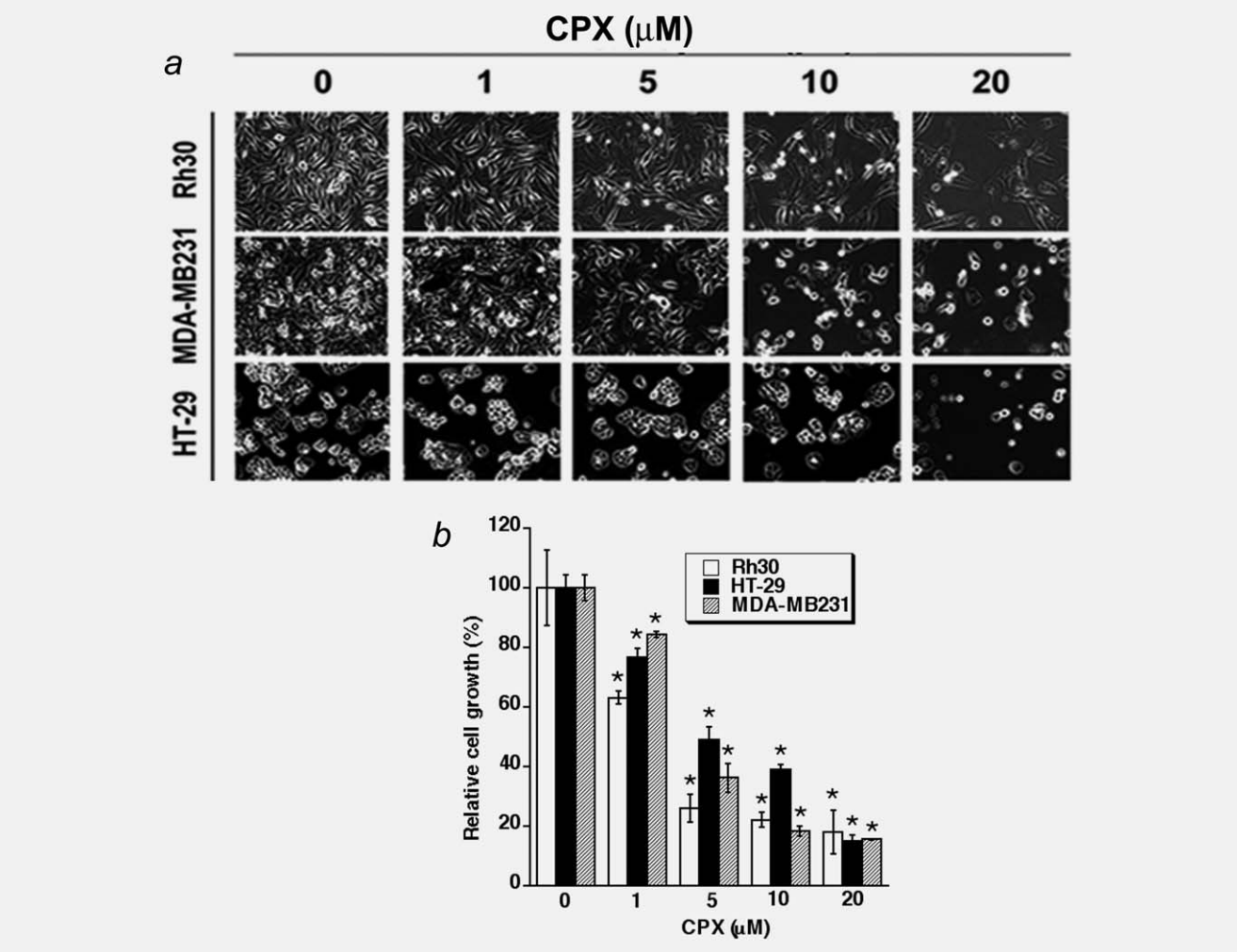

Figure 3. CPX inhibits proliferation of Rh30, MDA-MB231 and HT29 cells in a concentration-dependent manner. The indicated cells were treated with or without CPX (0–20 μM) for 48 days, followed by (*a*) morphological analysis or (*b*) cell proliferation assay, as described in Material and Methods. Results are presented as mean ± SD ($n = 3$). *$p < 0.05$, difference *versus* vehicle-treated control group.

$p27^{Kip1}$ expression concentration dependently (Fig. 6*b*). At 10–20 μM, CPX increased $p21^{Cip1}$ expression by 2- to 3-fold but decreased $p27^{Kip1}$ expression by 20–30%. In addition, time course studies revealed that CPX also increased $p21^{Cip1}$ expression but decreased $p27^{Kip1}$ expression time dependently (Fig. 6*b*). At 10 μM, CPX upregulated expression of $p21^{Cip1}$ rapidly. Even within 2-hr treatment, CPX increased $p21^{Cip1}$ expression by ~2-fold. After exposure to CPX for 16–24 hr, $p27^{Kip1}$ expression levels dropped by 20–30%.

CPX inhibits protein expression of Bcl-xL and survivin and increases cleavages of Bcl-2, resulting in apoptosis

Apoptosis is regulated by proapoptotic and antiapoptotic proteins.[21] To investigate the mechanism by which CPX induces apoptosis of tumor cells, we examined expression of antiapoptotic proteins (Bcl-xL, survivin and Bcl-2) and proapoptotic proteins (BAD, BAX and BAK). CPX did not obviously alter expression of BAD, BAX and BAK (data not shown) but markedly decreased levels of Bcl-xL and survivin and increased cleavage of Bcl-2 in a time- and concentration-dependent manner (Fig. 7*a*). In addition, treatment with CPX for 24 hr also dose dependently enhanced cleavage of PARP (Fig. 7*a*), indicating caspase-dependent apoptosis. The amount of cleaved PARP induced by 10 μM CPX at 24 hr was limited, which is consistent with very little apoptosis at this time point, as determined by the Annexin-V/PI staining (data not shown). However, treatment with 10 μM CPX for 48 hr was able to induce the same level of PARP cleavage or cell death as treatment with 20 μM CPX for 24 hr (data not shown).

To verify the role of caspases in CPX-induced cell death, Z-VAD-FMK, a pan-caspase inhibitor, was used. We observed that treatment of cells with 10 μM of Z-VAD-FMK almost completely blocked caspase-3/7 activity induced by CPX (5 and 20 μM) (Fig. 7*b*) and partially prevented CPX-induced cell death (Fig. 7*c*), suggesting that CPX-induced apoptosis of cancer cells is mediated in part through caspase-dependent mechanism.

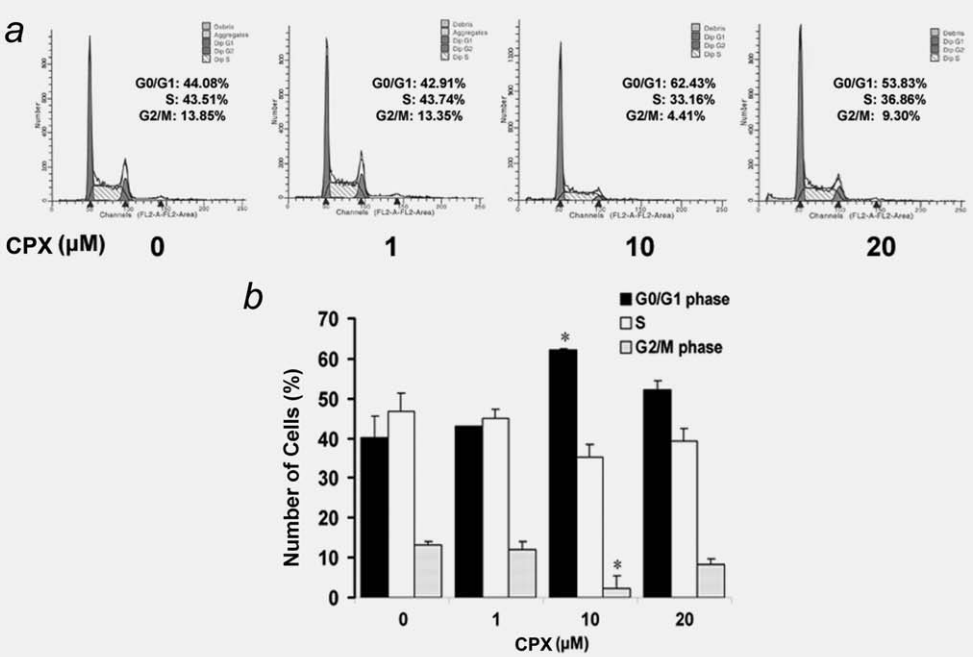

Figure 4. CPX induces G_1/G_0 cell cycle arrest in tumor cells. (*a*) Rh30 cells were treated without or with CPX (0–20 μM) for 24 hr. The cells were harvested and processed for cell cycle analysis using Cellular DNA Flow Cytometric Analysis Kit. (*b*) A summary of cell cycle distribution data in (*a*). Results are presented as mean ± SD ($n = 3$). *$p < 0.05$, difference *versus* vehicle-treated control group.

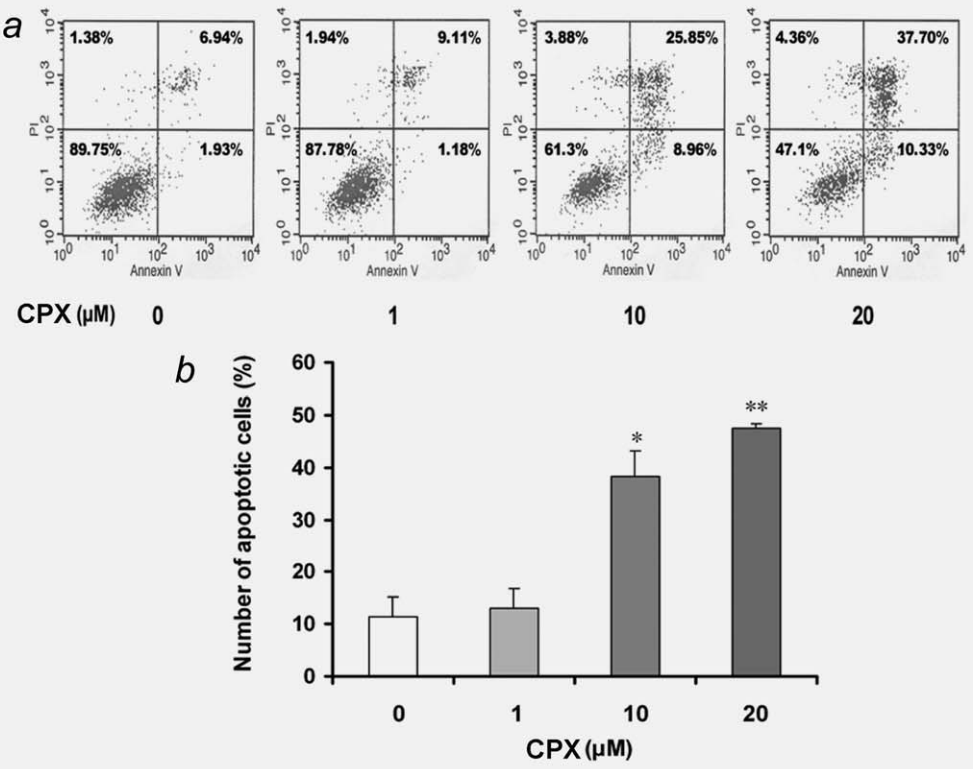

Figure 5. CPX induces apoptosis in tumor cells. (*a*) Rh30 cells were treated without or with CPX (0–20 μM) for 48 hr. The cells were harvested and processed for apoptosis assay using the Annexin V-FITC Apoptosis Detection Kit I. (*b*) A summary of total percent of apoptotic cells after CPX treatment for 48 hr. Results are presented as mean ± SD ($n = 3$). *$p < 0.05$, **$p < 0.01$, difference *versus* vehicle-treated control group.

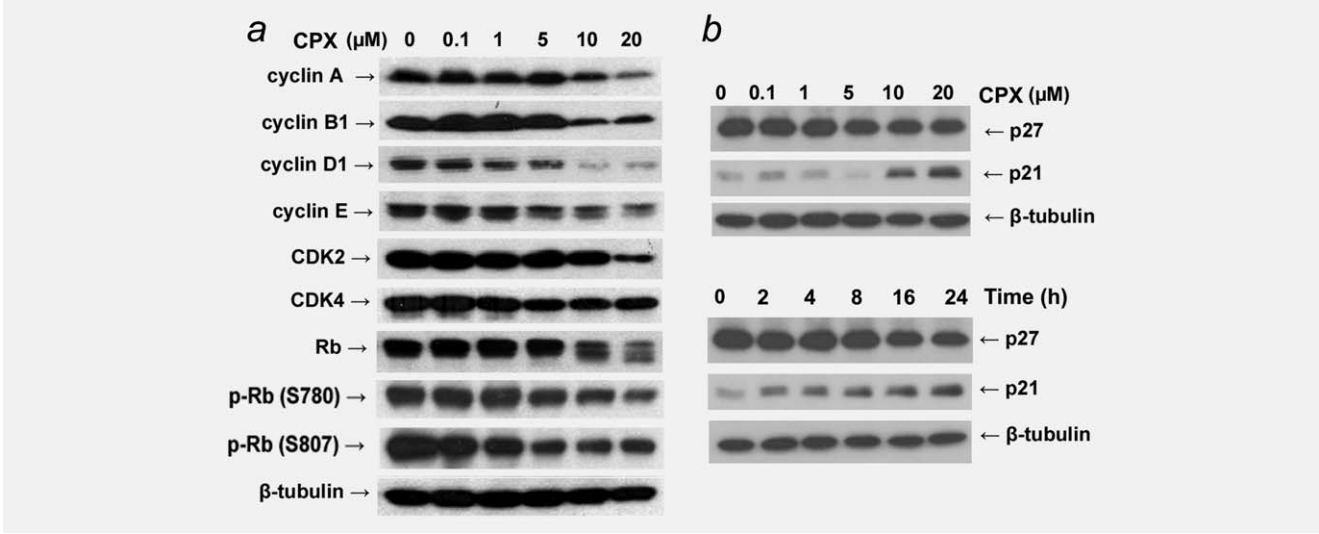

Figure 6. CPX downregulates expression of cyclins and CDKs and upregulates expression of $p21^{Cip1}$, leading inhibition of phosphorylation of Rb in tumor cells. (*a*) Rh30 cells were treated without or with CPX (0–20 μM) for 24 hr, the cells were harvested and cellular extracts were subjected to Western blot analysis. β-tubulin was used as a loading control. (*b*) Rh30 cells were treated with 10 μM of CPX for different time periods (0–24 hr) or with different concentration of CPX (0–20 μM) for 16 hr. The cells were harvested and subjected to Western blot analysis. β-tubulin was used as a loading control.

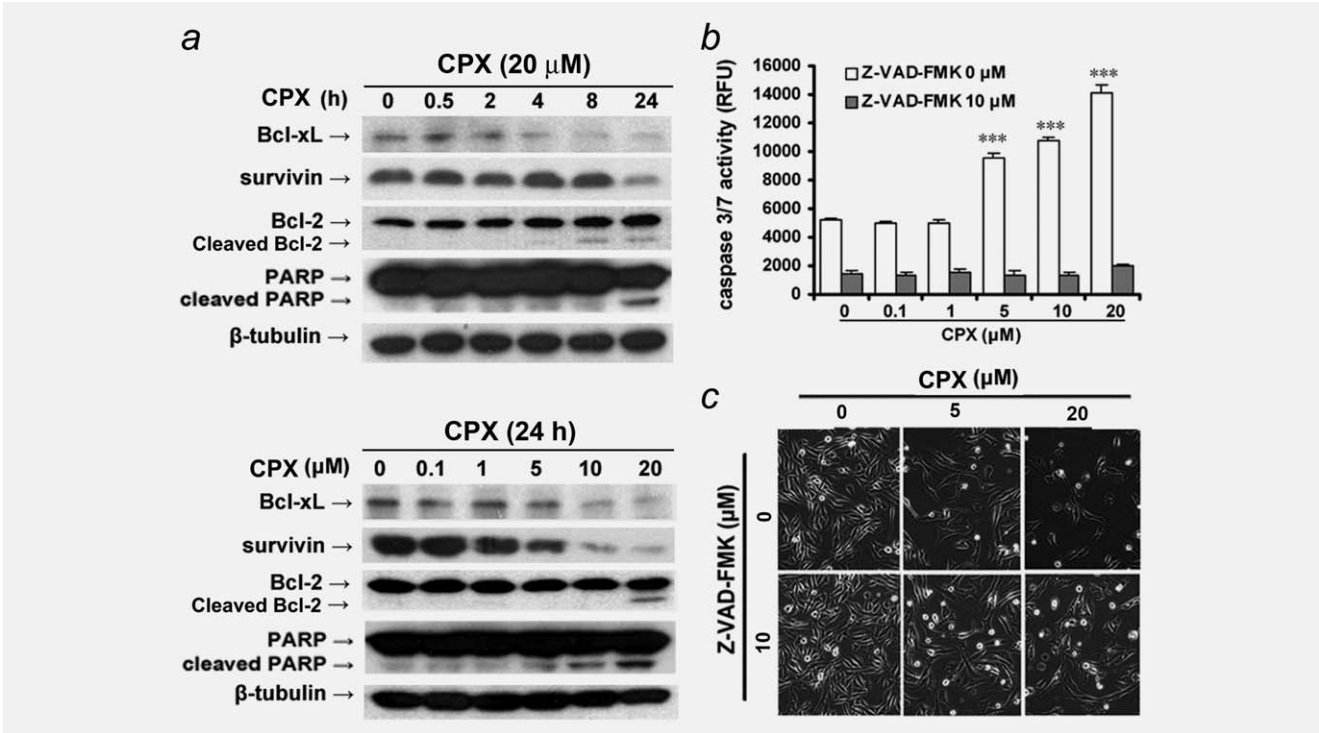

Figure 7. CPX downregulates expression of Bcl-xL and survivin and increases cleavage of Bcl-2, leading to caspase-dependent and -independent apoptosis in tumor cells. (*a*) Rh30 cells were treated with CPX (20 μM) for 0–24 hr or with CPX (0–20 μM) for 24 hr. The cells were harvested and subjected to Western blot analysis. β-tubulin was used as a loading control. (*b*) Rh30 cells, pretreated with or without Z-VAD-FMK (10 μM) for 30 min, were incubated with CPX (0–20 μM) for 24 hr, followed by caspase-3/7 activity assay as described in Material and Methods. (*c*) Rh30 cells were treated without or with CPX (5 or 20 μM) for 48 hr following preincubation with Z-VAD-FMK (10 μM) for 1 hr. The cells were photographed with an Olympus inverted phase-contrast microscope (×200) equipped with Quick Imaging System.

Discussion

Ciclopirox olamine is a synthetic antifungal agent and iron chelator, which has been used to treat mycoses of the skin and nails for over 2 decades.[1,2] However, little is known about its antitumor effect. Here, for the first time, we show that CPX inhibits tumor growth in human breast cancer MDA-MB231 xenografts, which is related to reduced proliferation and increased apoptosis of the tumor cells. This is supported by our Ki-67 staining and TUNEL assay data. Further, the antitumor effect of CPX is confirmed in the cell culture model, as CPX inhibits proliferation and induces apoptosis of human rhabdomyosarcoma (Rh30), breast carcinoma (MDA-MB231) and colon adenocarcinoma (HT-29) cells in culture. Our data strongly suggest that CPX is a potential antitumor agent. This is consistent with other findings that iron chelators, such as desferrioxamine,[22] Dp44mT[23–25] and ICRF-187,[26] may be exploited for cancer therapy.

It is well known that iron is essential for proliferation, DNA synthesis and repair, mitochondrial electron transport and oxygen sensing.[27] Cancer cells have higher requirement for iron because of faster proliferation.[27] Studies have shown that CPX inhibits the iron-dependent enzyme ribonucleotide reductase, which is involved in the synthesis of DNA.[12] CPX also inhibits the iron-containing enzymes, such as catalase and peroxidase,[11] which are critical for decomposition of hydrogen peroxide, one of the reactive oxygen species involved in oxidative stress.[28] Whether CPX functions as an anticancer agent through iron chelation remains to be determined.

In this study, we found that CPX inhibited cell proliferation by slowing down cell cycle progression from G_1/G_0 to S phase. This is, to some degree, consistent with previous findings that CPX arrests cells in G_1/G_0 phase in other mammalian cells,[7,8] but different from the data (G_2/M arrest) obtained from yeast *S. cerevisiae*.[9] Further studies are needed to address whether this is cell type dependent or is related to experimental conditions. In addition, we noticed that long-time (48–72 hr) exposure to higher concentrations (10–20 μM) of CPX caused more floating (dead) cells. Whether the cells are "arrested" or "dead" depend on the concentration and time of CPX treatment. It appears that cells "arrested" first and then died. It remains to be defined whether continued cell cycle progression from G_1/G_0 to S phase under the stress condition (presence of CPX) is related to the cell death.

Extensive studies have shown that eukaryotic cell cycle progression is regulated by a series of CDKs and cyclins.[15] During distinct phases of the cell cycle, cyclin/CDK complexes are formed and can guide the CDKs to appropriate substrates and activate their catalytic activity.[15] Early G_1 transition is mainly regulated by cyclin D complexed with CDK4 and/or CDK6, whereas late G_1-S and early S-phase transitions are regulated by cyclin E coupled with CDK2.[15,29,30] To further investigate how CPX accumulates cells in G_1/G_0 phase, we examined the effects of CPX on the expression of cell cycle regulatory proteins. Our Western blot analysis (Fig. 6) indicates that CPX downregulated protein expression of cyclin D1 and cyclin E1 as well as their enzymatic counterparts CDK4 and CDK2. In addition, CPX potently induced expression of a universal CDK inhibitor $p21^{Cip1}$, which can bind and inhibit the cyclin D-, E- and A-dependent kinases,[19] regulating the G_1 to S phase transition of the cell cycle, whereas CPX had no effect on expression of $p27^{Kip1}$. As all tumor cell lines used (Rh30, MDA-MB231 and HT-29) express mutant *p53* alleles, the results also indicate that CPX-induced $p21^{Cip1}$ expression is mediated through a p53-independent mechanism. Collectively, our data reveal that CPX downregulation of cyclins/CDKs and upregulation of $p21^{Cip1}$ may be responsible for accumulation of the cancer cells in G_1/G_0 cell cycle.

The Rb tumor-suppressor protein, a major target of CDKs, plays a pivotal role in the regulation of cell cycle progression from G_1 to S phase.[17] The activity of Rb is controlled by its phosphorylation status.[17] Hypophosphorylated Rb is the active growth-inhibitory form, which binds E2F and prevents G_1/S transition; in contrast, hyperphosphorylated Rb is released from E2F and is the inactive form.[31] The D cyclins and their counterparts CDKs have been suggested to be the most important regulators of Rb phosphorylation.[17,31] In this study, we observed a profound loss of Rb phosphorylation after a 24-hr exposure to CPX in Rh30 cells. The results suggest that CPX slowing down cell cycle progression from G_1/G_0 to S phase is a consequence of inhibition of Rb phosphorylation.

Here, we also found that CPX induces p53-independent apoptosis of tumor cells, as the tumor cell lines (Rh30, MDA-MB231 and HT-29) tested are all *p53* mutant. Mutations of *p53* have been documented in over 50% human tumors.[32] In our tumor xenograft studies, no obvious toxicity of CPX to the animals was seen, suggesting that CPX may represent a novel tumor-selective agent.

Apoptosis is a complex process that is tightly regulated by the balance of several proapoptotic proteins, such as Bax, Bad and BAK, as well as antiapoptotic proteins, such as Bcl-xL, Mcl-1 and survivin.[21] Our studies show that CPX inhibited expression of the antiapoptotic proteins Bcl-xL and survivin (Fig. 7), although it did not alter expression of the proapoptotic proteins, such as BAD, BAX and BAK. Recently, Bcl-2 was found to be cleaved by caspase-3 in cells undergoing apoptosis induced by Fas ligation, IL-3 withdrawal and alphavirus infection.[33,34] Of interest, the cleavage of Bcl-2 was demonstrated to be able to trigger cell death and may further activate downstream caspases, amplifying of the caspase cascade.[34] In this study, we found that Bcl-2 protein was cleaved during CPX-induced apoptotic cell death in Rh30 cells. Therefore, our data suggest that CPX-induced apoptosis is associated with downregulation of Bcl-xL and survivin as well as increased cleavage of Bcl-2.

Apoptosis could occur through caspase-dependent and -independent pathways.[35,36] We noticed that CPX induced

cleavage of PARP (Fig. 7), suggesting a caspase-dependent apoptotic mechanism involved. To confirm this, a pancaspase inhibitor, Z-VAD-FMK, was used in our study. We found that Z-VAD-FMK (10 μM) almost completely blocked CPX-induced caspase-3/7 activity and partially prevented CPX-induced cell death in Rh30 cells, implying that CPX-induced apoptosis of the cancer cells is at least in part mediated through caspase-dependent mechanism.

Finally, it should be noted that although our Ki-67 staining and TUNEL assay indicate that CPX inhibited MDA-MB231-xenografted tumor growth by inhibiting tumor proliferation and inducing apoptosis of the tumor cells, we still do not know whether these *in vivo* events were caused by downregulation of cyclins, CDKs, Bcl-xL and survivin and upregulation of CDK inhibitor $p21^{Cip1}$, as observed in cell culture. More investigations will be helpful to address this question.

In summary, we have shown that CPX inhibits tumor growth in human breast cancer MDA-MB231 xenografts. This is associated with its inhibition of cell proliferation and induction of apoptosis of tumor cells. In our cell culture model, mechanistically, CPX inhibition of cell proliferation is linked to its slowing down cell cycle progression from G_1/G_0 to S phase, which is due to downregulation of cyclins (A, B1, D1 and E) and CDKs (CDK2 and CDK4) and upregulation of CDK inhibitor $p21^{Cip1}$, resulting in hypophosphorylation of Rb. CPX induction of apoptosis is mainly related to downregulation of antiapoptotic proteins (Bcl-xL and survivin) and increased cleavage of Bcl-2, leading to apoptosis. CPX may be exploited as an antitumor agent.

Acknowledgements

This work was supported in part by NIH grant (S.H.), American Cancer Society Award (S.H.), Feist-Weiller Cancer Research Award (S.H.) and a Start-up Fund (S.H.) jointly from Louisiana State University Health Sciences Center in Shreveport, LA. The authors are grateful to Dr. Peter J. Houghton for providing Rh30 cells.

References

1. Jue SG, Dawson GW, Brogden RN. Ciclopirox olamine 1% cream. A preliminary review of its antimicrobial activity and therapeutic use. *Drugs* 1985;29: 330–41.
2. Bohn M, Kraemer KT. Dermatopharmacology of ciclopirox nail lacquer topical solution 8% in the treatment of onychomycosis. *J Am Acad Dermatol* 2000;43:S57–S69.
3. Dittmar W, Lohaus G. HOE 296, a new antimycotic compound with a broad antimicrobial spectrum. Laboratory results. *Arzneimittelforschung* 1973;23:670–4.
4. Abrams BB, Hanel H, Hoehler T. Ciclopirox olamine: a hydroxypyridone antifungal agent. *Clin Dermatol* 1991;9: 471–7.
5. Gupta AK. Ciclopirox: an overview. *Int J Dermatol* 2001;40:305–10.
6. Leem SH, Park JE, Kim IS, Chae JY, Sugino A, Sunwoo Y. The possible mechanism of action of ciclopirox olamine in the yeast *Saccharomyces cerevisiae*. *Mol Cells* 2003;15:55–61.
7. Farinelli SE, Greene LA. Cell cycle blockers mimosine, ciclopirox, and deferoxamine prevent the death of PC12 cells and postmitotic sympathetic neurons after removal of trophic support. *J Neurosci* 1996;16:1150–62.
8. Hoffman BD, Hanauske-Abel HM, Flint A, Lalande M. A new class of reversible cell cycle inhibitors. *Cytometry* 1991;12:26–32.
9. Almeida B, Sampaio-Marques B, Carvalho J, Silva MT, Leao C, Rodrigues F, Ludovico P. An atypical active cell death process underlies the fungicidal activity of ciclopirox olamine against the yeast *Saccharomyces cerevisiae*. *FEMS Yeast Res* 2007;7:404–12.
10. Sakai K, Suzuki K, Tanaka S, Koike T. Up-regulation of cyclin D1 occurs in apoptosis of immature but not mature cerebellar granule neurons in culture. *J Neurosci Res* 1999;58:396–406.
11. Niewerth M, Kunze D, Seibold M, Schaller M, Korting HC, Hube B. Ciclopirox olamine treatment affects the expression pattern of *Candida albicans* genes encoding virulence factors, iron metabolism proteins, and drug resistance factors. *Antimicrob Agents Chemother* 2003;47:1805–17.
12. Eberhard Y, McDermott SP, Wang X, Gronda M, Venugopal A, Wood TE, Hurren R, Datti A, Batey RA, Wrana J, Antholine WE, Dick J, et al. Chelation of intracellular iron with the antifungal agent ciclopirox olamine induces cell death in leukemia and myeloma cells. *Blood* 2009; 114:3064–73.
13. Alpermann HG, Schutz E. Studies on the pharmacology and toxicology of ciclopiroxolamine. *Arzneimittelforschung* 1981;31:1328–32.
14. Beevers CS, Li F, Liu L, Huang S. Curcumin inhibits the mammalian target of rapamycin-mediated signaling pathways in cancer cells. *Int J Cancer* 2006;119: 757–64.
15. Malumbres M, Barbacid M. Cell cycle, CDKs and cancer: a changing paradigm. *Nat Rev Cancer* 2009;9:153–66.
16. Vermeulen K, Van Bockstaele DR, Berneman ZN. The cell cycle: a review of regulation, deregulation and therapeutic targets in cancer. *Cell Prolif* 2003;36: 131–49.
17. Burkhart DL, Sage J. Cellular mechanisms of tumour suppression by the retinoblastoma gene. *Nat Rev Cancer* 2008; 8:671–82.
18. Sherr CJ, Roberts JM. CDK inhibitors: positive and negative regulators of G1-phase progression. *Genes Dev* 1999;13: 1501–12.
19. Xiong Y, Hannon GJ, Zhang H, Casso D, Kobayashi R, Beach D. p21 is a universal inhibitor of cyclin kinases. *Nature* 1993; 366:701–4.
20. Lee SJ, Ha MJ, Lee J, Nguyen P, Choi YH, Pirnia F, Kang WK, Wang XF, Kim SJ, Trepel JB. Inhibition of the 3-hydroxy-3-methylglutaryl-coenzyme A reductase pathway induces p53-independent transcriptional regulation of p21(WAF1/CIP1) in human prostate carcinoma cells. *J Biol Chem* 1998;273:10618–23.
21. Youle RJ, Strasser A. The BCL-2 protein family: opposing activities that mediate cell death. *Nat Rev Mol Cell Biol* 2008;9:47–59.
22. Santamaria D, Ortega S. Cyclins and CDKS in development and cancer: lessons from genetically modified mice. *Front Biosci* 2006;11:1164–88.
23. Buss JL, Torti FM, Torti SV. The role of iron chelation in cancer therapy. *Curr Med Chem* 2003;10:1021–34.
24. Yuan J, Lovejoy DB, Richardson DR. Novel di-2-pyridyl-derived iron chelators with marked and selective antitumor activity: in vitro and in vivo assessment. *Blood* 2004; 104:1450–8.
25. Whitnall M, Howard J, Ponka P, Richardson DR. A class of iron chelators with a wide spectrum of potent antitumor activity that overcomes resistance to chemotherapeutics. *Proc Natl Acad Sci USA* 2006;103:14901–6.
26. Rao VA, Klein SR, Agama KK, Toyoda E, Adachi N, Pommier Y, Shacter EB. The iron chelator Dp44mT causes DNA damage and selective inhibition of

topoisomerase IIalpha in breast cancer cells. *Cancer Res* 2009;69:948–57.
27. Cazzola M, Bergamaschi G, Dezza L, Arosio P. Manipulations of cellular iron metabolism for modulating normal and malignant cell proliferation: achievements and prospects. *Blood* 1990;75:1903–19.
28. Trachootham D, Alexandre J, Huang P. Targeting cancer cells by ROS-mediated mechanisms: a radical therapeutic approach? *Nat Rev Drug Discov* 2009;8: 579–91.
29. Barry EV, Vrooman LM, Dahlberg SE, Neuberg DS, Asselin BL, Athale UH, Clavell LA, Larsen EC, Moghrabi A, Samson Y, Schorin MA, Cohen HJ, Lipshultz SE, Sallan SE, Silverman LB. Absence of secondary malignant neoplasms in children with high-risk acute lymphoblastic leukemia treated with dexrazoxane. *J Clin Oncol* 2008;26:1106–11.
30. Lindqvist A, Rodriguez-Bravo V, Medema RH. The decision to enter mitosis: feedback and redundancy in the mitotic entry network. *J Cell Biol* 2009;185: 193–202.
31. Polager S, Ginsberg D. E2F—at the crossroads of life and death. *Trends Cell Biol* 2008;18:528–35.
32. Feng Z, Hu W, Rajagopal G, Levine AJ. The tumor suppressor p53: cancer and aging. *Cell Cycle* 2008;7:842–7.
33. Cheng EH, Kirsch DG, Clem RJ, Ravi R, Kastan MB, Bedi A, Ueno K, Hardwick JM. Conversion of Bcl-2 to a Bax-like death effector by caspases. *Science* 1997; 278:1966–8.
34. Grandgirard D, Studer E, Monney L, Belser T, Fellay I, Borner C, Michel MR. Alphaviruses induce apoptosis in Bcl-2-overexpressing cells: evidence for a caspase-mediated, proteolytic inactivation of Bcl-2. *EMBO J* 1998;17: 1268–78.
35. Kasibhatla S, Tseng B. Why target apoptosis in cancer treatment? *Mol Cancer Ther* 2003;2:573–80.
36. Tait SW, Green DR. Caspase-independent cell death: leaving the set without the final cut. *Oncogene* 2008;27: 6452–61.